

De Novo Design of Synthetic Di-Iron(I) Complexes as Structural Models of the Reduced Form of Iron–Iron Hydrogenase

Jesse W. Tye, Marcetta Y. Darensbourg,* and Michael B. Hall*

Department of Chemistry, Texas A&M University, College Station, Texas 77843-3255

Received July 24, 2005

Simple synthetic di-iron dithiolate complexes provide good models of the composition of the active site of the iron–iron hydrogenase enzymes. However, the formally Fe^IFe^I complexes synthesized to date fail to reproduce the precise orientation of the diatomic ligands about the iron centers that is observed in the molecular structure of the reduced form of the enzyme active site. This structural difference is often used to explain the fact that the synthetic di-iron complexes are generally poor catalysts when compared to the enzyme. Herein, density functional theory computations are used for the rational design of synthetic complexes as structural models of the reduced form of the enzyme active site. These computations suggest several possible synthetic targets. The synthesis of complexes containing five-atom S-to-S linkers of the form S(CH₂)₂X(CH₂)₂S (X = CH₂, NH, or O) or pendant functionalities attached to the three-carbon framework is one method. Another approach is the synthesis of asymmetrically substituted complexes, in which one iron center has strongly electron donating ligands and the adjacent iron center has strongly electron accepting ligands. The combination of a sterically demanding S-to-S linker and asymmetric substitution of the CO ligands is predicted to be a particularly effective synthetic target.

Introduction

Hydrogenase enzymes are used by many microorganisms in nature to facilitate the reversible oxidation of dihydrogen to protons and electrons, $\text{H}_2 \leftrightarrow 2\text{H}^+ + 2\text{e}^-$.^{1–3} The structurally characterized hydrogenase enzymes can be broadly divided into [NiFe]^{4–7} and [FeFe]^{8,9} hydrogenases on the basis of the metal content of their active sites. In nature, the [NiFe] enzymes generally function as hydrogen oxidation catalysts, while the [FeFe] enzymes generally catalyze the production of dihydrogen.

These enzymes are of considerable interest because of their potential uses in biotechnological applications.¹⁰ A major drawback is the fact that the organisms that produce hydrogenase enzymes are generally anaerobic extremophiles that require high temperatures, high pressures, and the exclusion of oxygen to live. The [NiFe] enzymes are generally considered more thermally and O₂ stable than the [FeFe] enzymes and, therefore, potentially more suitable to act as large-scale biocatalysts for H₂ oxidation and H⁺ reduction. On the other hand, the synthesis of small molecule analogues of the [FeFe] enzyme active site has proven to be more straightforward because of limited direct involvement of the protein in the enzyme active site and its resemblance to the previously known organometallic complex ($\mu\text{-S}(\text{CH}_2)_3\text{S}[\text{Fe}(\text{CO})_3]_2$).¹¹

Darensbourg, Pickett, Rauchfuss, and their respective co-workers have synthesized simple dinuclear iron complexes that have structural, spectroscopic, and functional properties similar to the active site of [FeFe]H₂ase. Darensbourg and co-workers have examined the ability of formal Fe^IFe^I complexes (synthetic analogues of the reduced form, known

* To whom correspondence should be addressed. E-mail: marcetta@mail.chem.tamu.edu (M.Y.D.), mbhall@tamu.edu (M.B.H.).

- (1) Nicolet, Y.; Cavazza, C.; Fontecilla-Camps, J. C. *J. Inorg. Biochem.* **2002**, *91*, 1–8.
- (2) Tamagnini, P.; Axelsson, R.; Lindberg, P.; Oxelfelt, F.; Wunschiers, R.; Lindblad, P. *Microbiol. Mol. Biol. Rev.* **2002**, *66*, 1–20.
- (3) Frey, M. *Structure and Bonding*; Springer-Verlag: Berlin, Heidelberg, **1998**, *90*, 98–126.
- (4) Przybyla, A. E.; Robbins, J.; Menon, N.; Peck, H. D., Jr. *FEMS Microbiol. Rev.* **1992**, *88*, 109–135.
- (5) Garcin, E.; Vernede, X.; Hatchikian, E. C.; Volbeda, A.; Frey, M.; Fontecilla-Camps, J. C. *Structure* **1999**, *7*, 557–566.
- (6) Teixeira, M.; Moura, I.; Xavier, A. V.; Moura, J. J. G.; LeGall, J.; DerVartanian, D. V.; Peck, H. D., Jr.; Huynh, B. H. *J. Biol. Chem.* **1989**, *264*, 16435–16450.
- (7) Volbeda, A.; Fontecilla-Camps, J. C. *Dalton Trans.* **2003**, 4030–4038.
- (8) Nicolet, Y.; Lemon, B. J.; Fontecilla-Camps, J. C.; Peters, J. W. *Trends Biochem. Sci.* **2000**, *25*, 138–143.
- (9) Peters, J. W. *Curr. Opin. Struct. Biol.* **1999**, *9*, 670–676.

- (10) Mertens, R.; Liese, A. *Curr. Opin. Biotechnol.* **2004**, *15*, 343–348.
- (11) Seyferth, D.; Womack, G. B.; Gallagher, M. K.; Cowie, M.; Hames, B. W.; Fackler, J. P., Jr.; Mazany, A. M. *Organometallics* **1987**, *6*, 283–294.

as H_{red}) to function as solution electrocatalysts for H_2 production in the presence of acid.^{12,13} Pickett and co-workers presented infrared spectral data for the formation of a short-lived $Fe^II Fe^I$ species derived from the oxidation of the Fe^I - Fe^I complex $[Fe_2\{MeSCH_2C(Me)(CH_2S)_2\}(CN)_2(CO)_4]^{2-}$.¹⁴ The resulting $Fe^II Fe^I$ complex contains a bridging CO ligand as evidenced by infrared spectroscopy, and the $\nu(CO)$ and $\nu(CN)$ values of this complex are very similar to those observed for the H_{ox} form of the active site of $[FeFe]-H_2ase$.^{15–17} Rauchfuss and co-workers have synthesized a series of $Fe^II Fe^II$ complexes that contain bridging CO ligands and serve as models of the H_{ox}^{air} form of the enzyme active site.¹⁸

The $Fe^I Fe^I$ complexes synthesized to date require much harsher conditions than those employed in the enzymatic catalysis to afford proton reduction. Direct electrochemistry performed on the $[FeFe]H_2ase$ enzyme from *Megasphaera elsdenii* shows that this enzyme catalyzes H_2 production at pH 7 and at a mild overpotential of -0.421 ± 0.010 V versus SHE (SHE = standard hydrogen electrode).¹⁹ In general, these complexes require reduction to the $Fe^I Fe^0$ or $Fe^0 Fe^0$ formal oxidation state to produce H_2 , while the enzyme apparently utilizes the $Fe^I Fe^I$ formal oxidation state. In addition, the $Fe^I Fe^I$ complexes synthesized to date require either strong acids (i.e., toluenesulfonic acid) and moderate overpotentials (≈ -1.0 to -1.2 V vs SHE)^{20–24} or weak acids (i.e., acetic acid) and even more negative overpotentials (≈ -1.3 to -1.9 V vs SHE) to produce H_2 .^{12,13}

The $Fe^I Fe^I$ complexes, synthesized to date, also fail to mimic the precise orientation of the diatomic ligands about the Fe_2S_2 core (Figure 1) that is observed in the reduced form of the enzyme.¹⁶ It may be that this unique orientation of the diatomic ligands about the distal iron of the active site of $[FeFe]H_2ase$ promotes H^+ acceptance. This unique structure may be due to a combination of the electronic effect of ligands bonded directly to the iron centers and specific interactions between the first and the second coordination spheres (such as hydrogen bonds between the cyanide

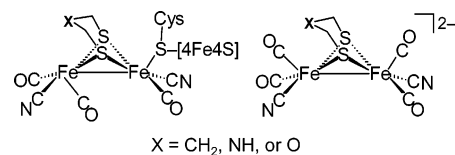


Figure 1. Comparison between the putative $Fe^I Fe^I$ form (H_{red}) of the active site of $[FeFe]H_2ase$ from *Desulfovibrio desulfuricans* (left) and closely related synthetic $Fe^I Fe^I$ complexes (right). The major structural difference is the placement of a CO ligand on the left-most iron in each complex (known as the distal iron in the enzyme).

nitrogens and the remainder of the protein). The precise placement and orientation of hydrogen bond donors observed in the protein is difficult to reproduce with small synthetic analogues. As an alternative strategy, changes to the primary coordination sphere of the synthetic compounds may be able to compensate for the lack of specific interactions provided by the protein.

Here, we use computational chemistry to design $Fe^I Fe^I$ complexes that more closely resemble the structure of the active site of $[FeFe]H_2ase$. Specifically, we determine modifications of S-to-S linker and donor ligands that act to stabilize a structure similar to that observed in the molecular structure of the enzyme active site. In this text, we will refer to structures in which one of the CO ligands resides in the area “between” the two iron centers, structures which more closely resemble the enzyme active site, as *rotated structures* and structures where the $Fe(CO)_2L$ units roughly eclipse one another with no ligand in the area “between” the two iron centers, as in all $Fe^I Fe^I$ complexes synthesized to date, as *unrotated structures*. Thus, we are trying to predict designs for abiotic, $Fe^I Fe^I$ complexes with the observed biological rotated structure. Previous computational work in this area has focused on the catalytic mechanism for H^+ reduction/ H_2 oxidation,^{25–31} the nature of the S-to-S linker in the enzyme active site,³² the electronic structure and reactivity of synthetic analogues of the $[FeFe]H_2ase$ active site,^{18,20,33–38} and factors that influence the active site structure.³⁹

Computational Details

All density functional theory (DFT) calculations were performed using a hybrid functional [the three-parameter exchange functional

- (12) Chong, D.; Georgakaki, I. P.; Mejia-Rodriguez, R.; Sanabria-Chinchilla, J.; Soriaga, M. P.; Darensbourg, M. Y. *Dalton Trans.* **2003**, 4158–4163.
- (13) Mejia-Rodriguez, R.; Chong, D.; Reibenspies, J. H.; Soriaga, M. P.; Darensbourg, M. Y. *J. Am. Chem. Soc.* **2004**, *126*, 12004–12014.
- (14) Razavet, M.; Borg, S. J.; George, S. J.; Best, S. P.; Fairhurst, S. A.; Pickett, C. J. *Chem. Commun.* **2002**, 700–701.
- (15) Lemon, B. J.; Peters, J. W. *Biochemistry* **1999**, *39*, 12969–12973.
- (16) Nicolet, Y.; de Lacey, A. L.; Vernede, X.; Fernandez, V. M.; Hatchikian, E. C.; Fontecilla-Camps, J. C. *J. Am. Chem. Soc.* **2001**, *123*, 1596–1601.
- (17) De Lacey, A. L.; Stadler, C.; Cavazza, C.; Hatchikian, E. C.; Fernandez, V. M. *J. Am. Chem. Soc.* **2000**, *122*, 11232–11233.
- (18) Boyke, C. A.; Rauchfuss, T. B.; Wilson, S. R.; Rohmer, M.-M.; Bénard, M. *J. Am. Chem. Soc.* **2004**, *126*, 15151–15160.
- (19) Butt, J. N.; Filipiak, M.; Hagen, W. R. *Eur. J. Biochem.* **1997**, *245*, 116–122.
- (20) Gloaguen, F.; Lawrence, J. D.; Rauchfuss, T. B.; Bénard, M.; Rohmer, M.-M. *Inorg. Chem.* **2002**, *41*, 6573–6582.
- (21) Ott, S.; Kritikos, M.; Åkermark, B.; Sun, L.; Lomoth, R. *Angew. Chem., Int. Ed.* **2004**, *43*, 1006–1010.
- (22) Capon, J.-F.; Gloaguen, F.; Schollhammer, P.; Talarmin, J. *J. Electroanal. Chem.* **2004**, *566*, 241–247.
- (23) Liu, T.; Wang, M.; Shi, Z.; Cui, H.; Dong, W.; Chen, J.; Åkermark, B.; Sun, L. *Chem.—Eur. J.* **2004**, *10*, 4474–4479.
- (24) Borg, S. J.; Behrsing, T.; Best, S. P.; Razavet, M.; Liu, X.; Pickett, C. J. *J. Am. Chem. Soc.* **2004**, *126*, 16988–16999.

- (25) Cao, Z.; Hall, M. B. *J. Am. Chem. Soc.* **2001**, *123*, 3734–3742.
- (26) Liu, Z.-P.; Hu, P. *J. Am. Chem. Soc.* **2002**, *124*, 5175–5182.
- (27) Dance, I. *Chem. Commun.* **1999**, 1655–1656.
- (28) Bruschi, M.; Fantucci, P.; De Gioia, L. *Inorg. Chem.* **2002**, *41*, 1421–1429.
- (29) Liu, Z.-P.; Hu, P. *J. Chem. Phys.* **2002**, *117*, 8177–8180.
- (30) Bruschi, M.; Fantucci, P.; De Gioia, L. *Inorg. Chem.* **2003**, *42*, 4773–4781.
- (31) Zhou, T.; Mo, Y.; Liu, A.; Zhou, Z.; Tsai, K. R. *Inorg. Chem.* **2004**, *43*, 923–930.
- (32) Fan, H.-J.; Hall, M. B. *J. Am. Chem. Soc.* **2001**, *123*, 3828–3829.
- (33) Lawrence, J. D.; Li, H.; Rauchfuss, T. B.; Bénard, M.; Rohmer, M.-M. *Angew. Chem., Int. Ed.* **2001**, *40*, 1768–1771.
- (34) Lyon, E. J.; Georgakaki, I. P.; Reibenspies, J. H.; Darensbourg, M. Y. *J. Am. Chem. Soc.* **2001**, *123*, 3268–3278.
- (35) Georgakaki, I. P.; Thomson, L. M.; Lyon, E. J.; Hall, M. B.; Darensbourg, M. Y. *Coord. Chem. Rev.* **2003**, *238–239*, 255–266.
- (36) Tard, C.; Liu, X.; Ibrahim, S. K.; Bruschi, M.; De Gioia, L.; Davies, S. C.; Yang, X.; Wang, L.-S.; Sawers, G.; Pickett, C. J. *Nature* **2005**, *434*, 610–613.
- (37) Zampella, G.; Bruschi, M.; Fantucci, P.; Razavet, M.; Pickett, C. J.; De Gioia, L. *Chem.—Eur. J.* **2005**, *11*, 509–533.
- (38) Fiedler, A. T.; Brunold, T. C. *Inorg. Chem.* **2005**, *44*, 1794–1809.

of Becke (B3)⁴⁰ and the correlation functional of Lee, Yang, and Parr (LYP)⁴¹] (B3LYP) as implemented in Gaussian 03.⁴² The iron, phosphorus, and sulfur atoms use the effective core potential and associated basis set of Hay and Wadt (LANL2DZ).^{43,44} For iron, the two outermost p functions were replaced by re-optimized 4p functions as suggested by Couty and Hall.⁴⁵ For sulfur and phosphorus, the basis set was augmented by the d polarization function of Höllwarth et al.⁴⁶ The carbon and hydrogen atoms of the dithiolate and bis-thiolate ligands and the hydrogen atoms of the PH₃ ligand use Dunning's double- ζ basis (D95).^{47,48} The CO and CN⁻ ligands and the BH_x ($x = 1, 2$), NH_x ($x = 1, 2$), and OH_x ($x = 0, 1$) components of the dithiolate bridges use Dunning's correlation-consistent polarized valence double- ζ basis set (cc-pVDZ).⁴⁹ Unless otherwise noted, all geometries are fully optimized and confirmed as minima or n -order saddle points by analytical frequency calculations at the same level.

Results and Discussion

Fundamental Properties of $(\mu\text{-SR})_2[\text{Fe}(\text{CO})_3]_2$. Knowledge of the different conformational isomers observed for the $(\mu\text{-SRS})[\text{Fe}(\text{CO})_3]_2$ and $(\mu\text{-SR})_2[\text{Fe}(\text{CO})_3]_2$ complexes is important to the following discussion. For the S-to-S linked complexes such as $(\mu\text{-SCH}_2\text{CH}(\text{R})\text{CH}_2\text{S})[\text{Fe}(\text{CO})_3]_2$ there are two conformations which differ in the orientation of the R group. These orientations will be labeled as the *up* and *down* orientations as shown in Figure 2a. For the $(\mu\text{-SR})_2[\text{Fe}(\text{CO})_3]_2$ complexes, three conformational isomers are possible, which differ in the orientation of the carbon atom α to the thiolate sulfur. These isomeric forms will be labeled as *anti*, *syn*, and *syn'* as shown in Figure 2b. For monosubstituted complexes such as $(\mu\text{-SRS})[\text{Fe}(\text{CO})_3][\text{Fe}(\text{CO})_2(\text{PH}_3)]$, there are two PH₃ positional isomers. These PH₃ positional isomers will be labeled as *apical* and *basal* isomers as shown in

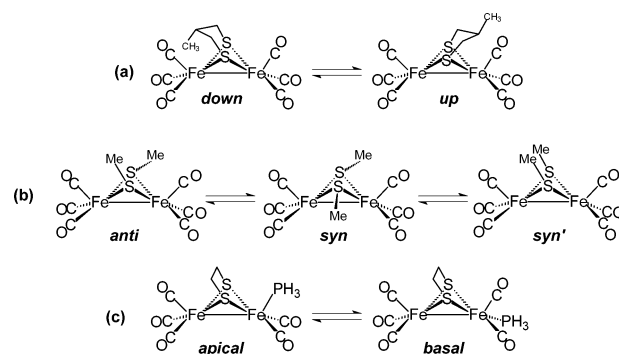


Figure 2. Intramolecular site-exchange processes in di-iron dithiolate and di-iron bis-thiolate complexes. (a) Dithiolate FeS₂C₃ ring inversion, (b) inversion at S, and (c) apical-basal exchange of the PH₃ ligand.

Scheme 1

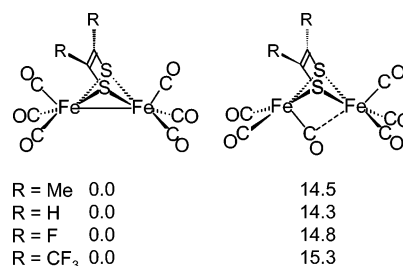


Figure 2c. In general, all of these isomeric forms have similar energies and readily interconvert at and below room temperature.

Design of the Dithiolate Linker: Electronic Effects. Electronic Effect in $(\mu\text{-SC}(\text{R})\text{C}(\text{R})\text{S})[\text{Fe}(\text{CO})_3]_2$. To determine how the electronic characteristics of the dithiolate linker might affect the energy difference between the most stable rotated form and the most stable unrotated form, the rotated and unrotated forms of a series of complexes, $(\mu\text{-SC}(\text{R})\text{C}(\text{R})\text{S})[\text{Fe}(\text{CO})_3]_2$ ($\text{R} = \text{CF}_3, \text{F}, \text{H}, \text{or } \text{CH}_3$), were geometry-optimized. The computed energy differences (Scheme 1) show no correlation to the electron donating ability of the R group as measured by its Hammett constant⁵⁰ and are very similar for the series ($\Delta G = 14.3\text{--}15.3 \text{ kcal mol}^{-1}$). The ethylenedithiolate framework was chosen for the S-to-S linker because it directs the steric bulk of the R groups away from the Fe(CO)₃ rotors, allowing one to determine the way in which the energy difference between the most stable rotated form and most stable unrotated form is affected by the electronic character of the S-to-S linker by minimizing competing steric effects. The energy difference between the most stable rotated form and the most stable unrotated form is shown to be invariant to the electron donating or accepting nature of the S-to-S linker.

Linked Versus Nonlinked Sulfurs. To determine how the electronic characteristics of the non S-to-S linked bis-thiolate affect the energy difference between the most stable rotated form and the most stable unrotated form, complexes of the form $(\mu\text{-SR})_2[\text{Fe}(\text{CO})_3]_2$ ($\text{R} = \text{CH}_3, \text{H}, \text{or } \text{F}$) were geometry optimized. Although the nature of the R group has a large effect on the relative energies of the *anti*, *syn*, and

(39) Bruschi, M.; Fantucci, P.; De Gioia, L. *Inorg. Chem.* **2004**, *43*, 3733–3741.

(40) Becke, A. D. *J. Chem. Phys.* **1993**, *98*, 5648–5652.

(41) Lee, C. Yang, W. Parr, R. G. *Phys. Rev. B: Condens. Matter* **1988**, *37*, 785–789.

(42) Frisch, M. J.; Trucks, G. W.; Schlegel, H. B.; Scuseria, G. E.; Robb, M. A.; Cheeseman, J. R.; Montgomery, J. A., Jr.; Vreven, T.; Kudin, K. N.; Burant, J. C.; Millam, J. M.; Iyengar, S. S.; Tomasi, J.; Barone, V.; Mennucci, B.; Cossi, M.; Scalmani, G.; Rega, N.; Petersson, G. A.; Nakatsuji, H.; Hada, M.; Ehara, M.; Toyota, K.; Fukuda, R.; Hasegawa, J.; Ishida, M.; Nakajima, T.; Honda, Y.; Kitao, O.; Nakai, H.; Klene, M.; Li, X.; Knox, J. E.; Hratchian, H. P.; Cross, J. B.; Bakken, V.; Adamo, C.; Jaramillo, J.; Gomperts, R.; Stratmann, R. E.; Yazyev, O.; Austin, A. J.; Cammi, R.; Pomelli, C.; Ochterski, J. W.; Ayala, P. Y.; Morokuma, K.; Voth, G. A.; Salvador, P.; Dannenberg, J. J.; Zakrzewski, V. G.; Dapprich, S.; Daniels, A. D.; Strain, M. C.; Farkas, O.; Malick, D. K.; Rabuck, A. D.; Raghavachari, K.; Foresman, J. B.; Ortiz, J. V.; Cui, Q.; Baboul, A. G.; Clifford, S.; Cioslowski, J.; Stefanov, B. B.; Liu, G.; Liashenko, A.; Piskorz, P.; Komaromi, I.; Martin, R. L.; Fox, D. J.; Keith, T.; Al-Laham, M. A.; Peng, C. Y.; Nanayakkara, A.; Challacombe, M.; Gill, P. M. W.; Johnson, B.; Chen, W.; Wong, M. W.; Gonzalez, C.; Pople, J. A. *Gaussian 03*, revision B.05; Gaussian, Inc.: Wallingford, CT, 2004.

(43) Hay, P. J.; Wadt, W. R. *J. Chem. Phys.* **1985**, *82*, 284–298.

(44) Hay, P. J.; Wadt, W. R. *J. Chem. Phys.* **1985**, *82*, 270–283.

(45) Couty, M.; Hall, M. B. *J. Comput. Chem.* **1996**, *17*, 1359–1370.

(46) Höllwarth, A.; Böhme, M.; Dapprich, S.; Ehlers, A. W.; Gobbi, A.; Jonas, V.; Köhler, K. F.; Stegmann, R.; Veldkamp, A.; Frenking, G. *Chem. Phys. Lett.* **1993**, *208*, 237–240.

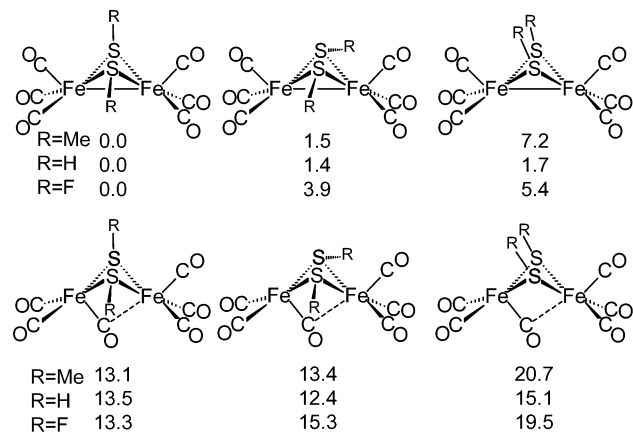
(47) Dunning, T. H., Jr.; Hay, P. J. In *Methods of Electronic Structure Theory*; Schaefer, H. F., III, Ed.; Plenum Press: New York, 1977; Vol. 3.

(48) Dunning, T. H., Jr. *J. Chem. Phys.* **1970**, *53*, 2823–2833.

(49) Dunning, T. H., Jr. *J. Chem. Phys.* **1989**, *90*, 1007–1023.

(50) Lowry, T. H.; Richardson, K. S. *Mechanism and Theory in Organic Chemistry*, 3rd ed.; Harper & Row: New York, 1987.

Scheme 2

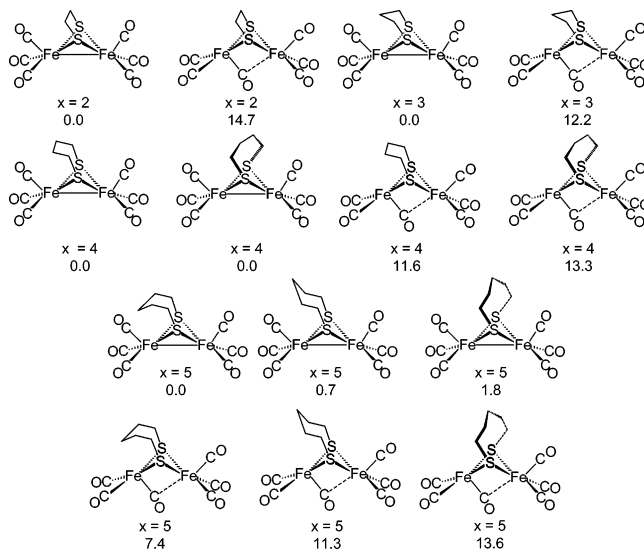


syn' isomers, the energy difference between the most stable rotated structure and the most stable unrotated structure is similar for all of these complexes (Scheme 2). Therefore, the energy difference between the most stable rotated form and the most stable unrotated form for non-S-to-S linked complexes of the type $(\mu\text{-SR})_2[\text{Fe}(\text{CO})_3]_2$ are also unrelated to the electron-donating or -accepting ability of the R group.

It is useful to compare the isomeric forms of nonlinked $(\mu\text{-SCH}_3)_2[\text{Fe}(\text{CO})_3]_2$ with the closely related S-to-S linked $(\mu\text{-S}(\text{CH}_2)_2\text{S})[\text{Fe}(\text{CO})_3]_2$ complex. The $(\mu\text{-S}(\text{CH}_2)_2\text{S})[\text{Fe}(\text{CO})_3]_2$ complex has a computed energy difference between the most stable rotated form and most stable unrotated form of 14.7 kcal mol⁻¹. The difference between the most stable rotated form and most stable unrotated form is 13.1 kcal mol⁻¹ for $(\mu\text{-SCH}_3)_2[\text{Fe}(\text{CO})_3]_2$. Therefore, the nonlinked complexes lead to a small relative stabilization of the rotated structures with respect to the unrotated structures.

S(CH₂)_xS Linkers (x = 2, 3, 4, or 5). To determine the role of the length of the dithiolate linker in the stabilization or destabilization of the rotated structure, the rotated and unrotated forms of a series of complexes $(\mu\text{-S}(\text{CH}_2)_x\text{S})[\text{Fe}(\text{CO})_3]_2$ (x = 2–5; Scheme 3) were geometry optimized. For the x = 3 complex and certain conformations of the dithiolate linker for the x = 4 and x = 5 complexes, the two Fe(CO)₃ rotors are inequivalent. The energy differences between the most stable rotated form and the most stable unrotated form for the less hindered end of the molecule (the Fe(CO)₃ unit furthest from the central methylene unit(s) of the dithiolate linker) are very similar to one another for the x = 3–5 species and the x = 2 species. The energy difference between the most stable rotated form and the most stable unrotated form of the more hindered end of the molecule (the Fe(CO)₃ unit nearest to the central methylene unit(s) of the dithiolate linker) is shown to be directly related to the length of the S-to-S linker. Increasing the length of the S-to-S linker leads to an increased steric repulsion between the nearby apical CO ligand and the central methylene unit(s) of the S-to-S linker in the unrotated structure. This steric repulsion is alleviated by rotation of the Fe(CO)₃ unit, leading to a lower relative energy for the rotated structures. In addition, the longer S-to-S linkers may also allow the formation of a stabilizing agostic interaction between the hydrogen atoms of the bridge and the “open site” present on the iron center

Scheme 3



in the rotated structures. The longer S-to-S linker alone lowers the energy difference between the most stable rotated form and most stable unrotated form from 14.7 kcal mol⁻¹ for the x = 2 complex down to 7.4 kcal mol⁻¹ for the x = 5 complex.

The replacement of one or more of the hydrogen atoms of S-to-S linker by larger alkyl groups should further destabilize the apical ligands of the unrotated forms. The x = 3 linker provides the best framework for the addition of steric bulk. Figure 3 compares the geometry optimized structures for x = 3 and x = 5 complexes. For the x = 3 complex, either orientation of the central methylene unit of the S-to-S linker places it near one of the apical CO ligands. The substitution of the central hydrogen atoms of the x = 3 by larger groups will result in destabilization of the apical CO of the unrotated form. The situation for the x = 5 complex is quite different. While certain conformations of the x = 5 complex direct the central methylene groups of the bridge toward the apical CO, low energy transition states convert these structures into other low energy structures which direct the steric bulk away from the apical CO. For the x = 5 linker, the steric interaction with the apical ligands

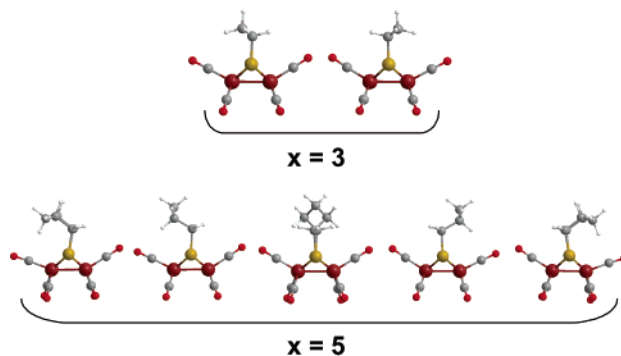
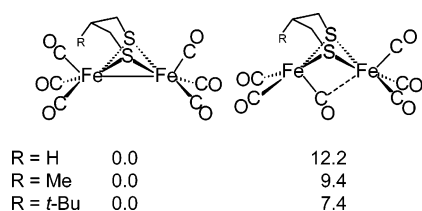
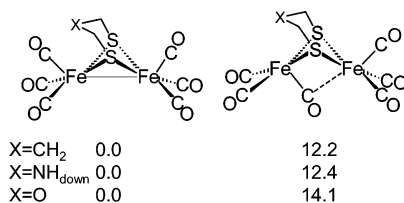


Figure 3. DFT-optimized structures for the $(\mu\text{-S}(\text{CH}_2)_x\text{S})[\text{Fe}(\text{CO})_3]_2$ series for x = 3, 5. Either orientation of the x = 3 bridge places the central methylene unit near one of the apical CO ligands. While some orientations of the x = 5 bridge places the central methylene units near one of the apical CO ligands, other structures, which are computed to have comparable energies, orient the central methylene groups away from either apical CO ligand.

Scheme 4



Scheme 5

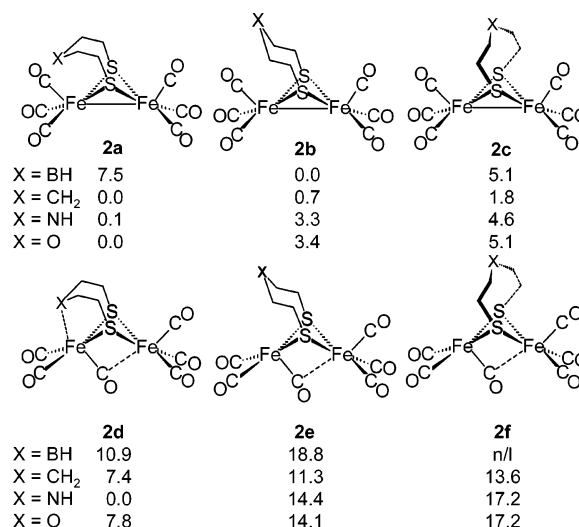


can be easily relieved by reorienting the S-to-S linker. Therefore, the $x = 4$ (not shown in Figure 3) and $x = 5$ linkers provide a poor framework for forcing a strong interaction with the apical CO ligand.

SCH₂CH(R)CH₂S Linkers. To determine the role of the steric bulk of the S-to-S linker in the stabilization or destabilization of the rotated structure, the rotated and unrotated forms of a series of complexes, $(\mu\text{-SCH}_2\text{CH(R)-CH}_2\text{S})[\text{Fe}(\text{CO})_3]_2$, were geometry-optimized. Two conformations are possible for the S-to-S linker in complexes of this form (Scheme 4). The “down” conformation directs the R group down and toward one of the Fe(CO)₃ units, while the “up” conformation directs the R group up and away from the Fe(CO)₃ units. For the down orientation of the R group, the energy difference between the most stable rotated form and the most stable unrotated form decreases as the steric bulk of the R group increases. Surprisingly, even the sterically demanding *tert*-butyl group does not force the rotated structure to be lower in energy. Instead, the Fe(CO)₃ unit tips away from the *tert*-butyl group to ease this interaction. The energy difference between the most stable rotated form and the most stable unrotated form is nearly invariant to the nature of the R group for the up orientation of the R group.

SCH₂XCH₂S Linkers. The identity of the central atom(s) of three-atom dithiolate linkers of the form SCH₂XCH₂S (X = CH₂, NH_{down}, or O) has very little effect on the energy difference between the most stable rotated form and the most stable unrotated form (as shown in Scheme 5). (We were unable to optimize a structure in which the NH hydrogen was oriented up. Multiple attempts at the geometry optimization of an NH_{up} species resulted in optimization of the NH_{down} species. This phenomenon has been observed and discussed previously.³³) The three-atom bridge directs the central atom(s) of the bridge away from the apical ligands in the unrotated structures and away from the iron center in the rotated structures. The rigid structure of these bridges limits the central atom(s) ability to destabilize the unrotated structures and/or to stabilize the rotated structures. The energy differences between the rotated and the unrotated structures of the X = CH₂ and X = NH_{down} species are slightly smaller than that of the X = O species, because the

Scheme 6



hydrogen atom of the central X = CH₂ and X = NH species destabilizes the apical CO of the unrotated structures.

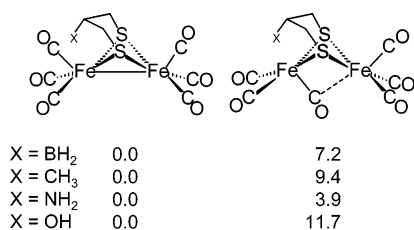
S(CH₂)₂X(CH₂)₂S Linkers. The identity of the central atom(s) of dithiolate linkers of the form S(CH₂)₂X(CH₂)₂S (X = BH, CH₂, NH, or O) has a dramatic effect on the energy difference between the most stable rotated form and the most stable unrotated form (as shown in Scheme 6). The five-atom bridge allows the central atom(s) of the bridge to interact strongly with the apical CO in the unrotated structures and/or the iron center in the rotated structures. The X = CH₂ and X = O complexes give similar results. The lowest energy structures **2a**-CH₂ and **2a**-O place the central CH₂ or O close to one of the apical CO ligands. Related structures in which the central CH₂ or O (**2b**-CH₂ and **2b**-O) is oriented away from the apical CO and the C₂ symmetric structures (**2c**-CH₂ and **2c**-O) are slightly less stable. The most stable rotated structures (**2d**-CH₂ and **2d**-O) have short Fe-X distances and μ -CO, but are still 7.4–7.8 kcal mol⁻¹ less stable than **2a**. The **2d**-CH₂ and **2d**-O complexes are shown by vibrational analysis (frequency calculations) to be minima on the B3LYP potential energy surface.

The X = BH complex has the largest energy difference between the most stable rotated structure and the most stable unrotated structure for this series of five-atom S-to-S linked complexes (10.9 kcal mol⁻¹). As with the other species the most stable rotated structure is **2d**-BH, which has a bridging CO ligand and a short Fe-B distance, but in contrast to the other species the most stable structural isomer of the unrotated form is **2b**-BH.

For X = NH the most stable structure, **2d**-NH, corresponds to the one which has a short Fe-N distance (NH_{up}) and a bridging CO ligand. This structure represents a minima on the potential energy surface as indicated by vibrational analysis. This result is markedly different from those found for the X = BH, CH₂, or O. The **2a**-NH complex is nearly isoenergetic with this species. The energies of the other relevant species are given in Scheme 6.

SCH₂CH(X)CH₂S Linkers: Pendant Functionalities. The nature of the pendant group attached to the central atom of the three-carbon S-to-S linker has a dramatic effect on

Scheme 7



difference in energy between the rotated and the unrotated structures (as shown in Scheme 7). For X = BH₂ and X = CH₃, the energy differences are 7.2 and 9.4 kcal mol⁻¹. Pendant NH₂ and OH groups give energies of 3.9 and 11.7 kcal mol⁻¹ for the rotated, μ -CO structures relative to the energies of the respective unrotated structures. Vibrational analysis shows that the rotated, μ -CO structures for X = NH₂ and X = OH correspond to minima on the B3LYP potential energy surface.

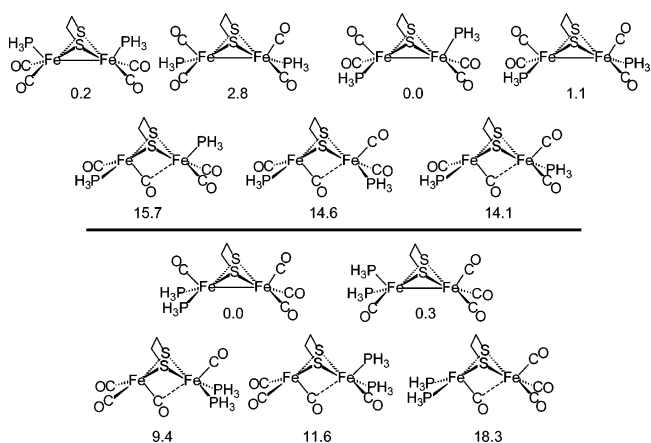
Ligand Effects: Monosubstituted Complexes. We³⁵ and others³⁹ have discussed the role of the donor strength of non-CO ligands in stabilizing structures of small molecule analogues that resemble those of the enzyme active site. We found that Fe(CO)₃ rotation in (μ -S(CH₂)₃S)[Fe(CO)₃]₂ induces the transfer of electron density from the unrotated Fe(CO)₃ unit to the rotated Fe(CO)₃ unit. In this context, the replacement of CO by a better donor ligand, L, facilitates the rotation of the Fe(CO)₃ unit and hinders the rotation of the Fe(CO)₂L unit. The replacement of CO by a poorer donor ligand than CO, L', facilitates the rotation of the Fe(CO)₂L' unit and hinders the rotation of the adjacent Fe(CO)₃ unit.

Oxidized and Reduced Species. The frontier molecule orbitals of the (μ -S(CH₂)₂S)[Fe(CO)₃]₂ complex are the highest occupied molecular orbital, which is primarily Fe–Fe bonding in nature, and the lowest unoccupied molecular orbital, which is primarily Fe–Fe antibonding in nature. The addition or removal of one electron from this complex will reduce the Fe–Fe bond order from 1 to 1/2 and, therefore, weaken the Fe–Fe bond.

Because the rotation of the Fe(CO)₃ unit of (μ -S(CH₂)₂S)[Fe(CO)₃]₂ requires breaking the Fe–Fe bond, the energy difference between the most stable rotated form and the most stable unrotated form is lowered by the addition or removal of electrons from (μ -S(CH₂)₂S)[Fe(CO)₃]₂. The neutral (μ -S(CH₂)₂S)[Fe(CO)₃]₂ complex has a computed energy difference between the most stable rotated form and the most stable unrotated form of 14.7 kcal mol⁻¹. The rotated structures of the one-electron reduced complex, [(μ -S(CH₂)₂S)[Fe(CO)₃]₂]¹⁻, and one-electron oxidized complex, [(μ -S(CH₂)₂S)[Fe(CO)₃]₂]¹⁺, are respectively 8.0 and 1.4 kcal mol⁻¹ less stable than the unrotated structures. For the two-electron oxidized complex, [(μ -S(CH₂)₂S)[Fe(CO)₃]₂]²⁺, the rotated structure is 8.8 kcal mol⁻¹ more stable than the unrotated structure. These results are not unexpected since Pickett, Rauchfuss, and their respective co-workers have synthesized Fe^{II}Fe^{II} and Fe^{II}Fe^I complexes, which contain bridging CO ligands.^{14,18}

Additivity. Ligand Effects: Disubstituted Complexes. A series of bis-PH₃ complexes of the forms (μ -S(CH₂)₂S)-

Scheme 8



[Fe(CO)₂(PH₃)₂] and (μ -S(CH₂)₂S)[Fe(CO)₃][Fe(CO)(PH₃)₂] and their respective Fe(CO)₃, Fe(CO)₂(PH₃), and Fe(CO)(PH₃)₂ rotated structures are given in Scheme 8. For the symmetrically substituted bis-PH₃ complexes of the form (μ -S(CH₂)₂S)[Fe(CO)₂(PH₃)₂], the most stable rotated structure lies at 14.1 kcal mol⁻¹ relative to the most stable unrotated structure. This value is larger than the energy difference between the most stable rotated form and the most stable unrotated form for mono-PH₃ complexes, (μ -S(CH₂)₂S)[Fe(CO)₃][Fe(CO)₂(PH₃)], (12.6 kcal mol⁻¹) and comparable to the value of 14.7 kcal mol⁻¹ computed for the all-CO complex (μ -S(CH₂)₂S)[Fe(CO)₃]₂, as a result of the symmetric substitution pattern of the PH₃ ligands. For the asymmetrically substituted bis-PH₃ complexes (μ -S(CH₂)₂S)[Fe(CO)₃][Fe(CO)(PH₃)₂], the most stable rotated structure lies at 9.4 kcal mol⁻¹ relative to the most stable unrotated structure. The difference in these structural isomers lies in the substitution pattern. In the mono-PH₃ complex, the transfer of electron density from the [Fe(CO)₂(PH₃)₂] unit stabilizes rotation of the adjacent Fe(CO)₃ unit. The substitution of one of the CO ligands of the Fe(CO)₂(PH₃) unit to yield the asymmetrically substituted (μ -S(CH₂)₂S)[Fe(CO)₃][Fe(CO)(PH₃)₂] complexes lowers the relative energy of the Fe(CO)₃ rotated structures relative to the unrotated structures by further facilitating the transfer of electron density from the Fe(CO)(PH₃)₂ unit into the adjacent Fe(CO)₃ unit. Symmetrical substitution of the PH₃ ligand stifles the transfer of electron density between the two iron centers.

Additivity. Combination of Ligand and Linker Effects. With the exception of oxidation or reduction, the most stabilizing modifications for the Fe^IFe^I complexes were the addition of a borane or amine functionality, the addition of a tertiary butyl group to the central methylene unit of the propanedithiolate linker, and the substitution of the CO ligand by a better donor ligand, L, to yield asymmetric complexes of the forms (μ -SRS)[Fe(CO)₃][Fe(CO)₂L] and (μ -SRS)[Fe(CO)₃][Fe(CO)L₂].

The replacement of CO by better donor ligands and the amine functionalized bridges are incompatible for the stabilization of the rotated form. The amine-functionalized bridge lowers the relative energy of the rotated structures by donating electron density to stabilize the “open site” created upon the Fe center by Fe(CO)₃ rotation. A good

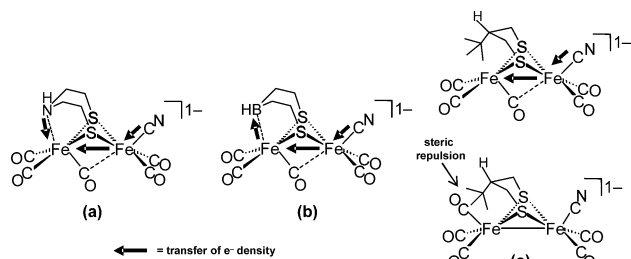


Figure 4. Combination of Effects. In parts a–c, the CN^- ligand stabilizes the rotated structure by making the unrotated $\text{Fe}(\text{CO})_2(\text{CN})$ unit a better donor to the rotated $\text{Fe}(\text{CO})_3$ unit. In part a, the amine nitrogen atom competes with the $\text{Fe}(\text{CO})_2(\text{CN})$ unit to donate into the rotated $\text{Fe}(\text{CO})_3$ unit. In part b, the borane makes the $\text{Fe}(\text{CO})_3$ unit a better electron density acceptor. In part c, the unrotated form is destabilized by the interaction with the tertiary butyl group.

donor ligand, L, also lowers the relative energy of the rotated structures by making the unrotated $\text{Fe}(\text{CO})_2\text{L}$ unit a better electron donor to the rotated $\text{Fe}(\text{CO})_3$ unit (Figure 4a). When both the amine functionalized bridge and a good donor ligand are present in the same complex, they compete for donation into the rotated $\text{Fe}(\text{CO})_3$ unit. For the all-CO complex $(\mu\text{-S}(\text{CH}_2)_2\text{NH}(\text{CH}_2)_2\text{S})[\text{Fe}(\text{CO})_3]_2$, the most stable rotated structure and most stable unrotated structure are isoenergetic. The most stable rotated structure and most stable unrotated structure remain isoenergetic for the mono-cyanide complex, $[(\mu\text{-S}(\text{CH}_2)_2\text{NH}(\text{CH}_2)_2\text{S})[\text{Fe}(\text{CO})_3][\text{Fe}(\text{CO})_2(\text{CN})]]^{1-}$. The replacement of one CO ligand of $(\mu\text{-S}(\text{CH}_2)_2\text{NH}(\text{CH}_2)_2\text{S})[\text{Fe}(\text{CO})_3]_2$ by CN^- , therefore, imparts no additional stabilization to the amine-stabilized rotated structures.

The replacement of CO by better donor ligands and the borane functionalized bridges are compatible for the stabilization of the rotated form. The borane-functionalized bridge lowers the relative energy of the rotated structures by making the rotated $\text{Fe}(\text{CO})_3$ unit a better electron acceptor (Figure 4b). A good donor ligand, L, lowers the relative energy of the rotated structures by making the unrotated $\text{Fe}(\text{CO})_2\text{L}$ unit a better electron donor to the rotated $\text{Fe}(\text{CO})_3$ unit. When both the borane functionalized bridge and a good donor ligand are present in the same complex, they cooperate to facilitate the transfer of electron density from the unrotated $\text{Fe}(\text{CO})_2\text{L}$ unit into the rotated $\text{Fe}(\text{CO})_3$ unit. The energy difference between the most stable rotated form and the most stable unrotated form is $10.9 \text{ kcal mol}^{-1}$ for the all-CO complex $(\mu\text{-S}(\text{CH}_2)_2\text{BH}(\text{CH}_2)_2\text{S})[\text{Fe}(\text{CO})_3]_2$. The energy difference between the most stable rotated form and the most stable unrotated form is $2.4 \text{ kcal mol}^{-1}$ for the mono-cyanide complex, $[(\mu\text{-S}(\text{CH}_2)_2\text{BH}(\text{CH}_2)_2\text{S})[\text{Fe}(\text{CO})_3][\text{Fe}(\text{CO})_2(\text{CN})]]^{1-}$. The replacement of one CO ligand of $(\mu\text{-S}(\text{CH}_2)_2\text{BH}(\text{CH}_2)_2\text{S})[\text{Fe}(\text{CO})_3]_2$ by CN^- , therefore, imparts additional stabilization to the borane-stabilized rotated structures.

The replacement of CO by better donor ligands and addition of steric bulk to the propanedithiolate framework are compatible for the stabilization of the rotated form. The addition of steric bulk to the propanedithiolate bridge destabilizes the unrotated forms by forcing a strong steric repulsion between the bridge and the apical ligands of the unrotated structures. A good donor ligand, L, stabilizes the rotated structures by making the unrotated $\text{Fe}(\text{CO})_2\text{L}$ unit a

better electron donor to the rotated $\text{Fe}(\text{CO})_3$ unit. These two factors work together to lower the relative energy of the rotated structures with respect to the unrotated structures (Figure 4c). The energy difference between the rotated and unrotated structures for the down orientation of the *tert*-butyl group of the all-CO complex $(\mu\text{-SCH}_2\text{C}(\text{t-Bu})\text{HCH}_2\text{S})[\text{Fe}(\text{CO})_3]_2$ is $7.4 \text{ kcal mol}^{-1}$. The replacement of one CO ligand by CN^- to yield the monocyanide complex, $[(\mu\text{-SCH}_2\text{C}(\text{t-Bu})\text{HCH}_2\text{S})[\text{Fe}(\text{CO})_3][\text{Fe}(\text{CO})_2(\text{CN})]]^{1-}$, lowers this value to $1.9 \text{ kcal mol}^{-1}$.

Conclusions

For a synthetic complex with the rotated structure to be isolated experimentally, at least one conformation of the rotated form must be more stable than the most stable conformation of the unrotated form. For this reason, all conformations of a given dithiolate bridge, anti, syn, and syn' orientations of bis-thiolates, and all possible orientations of the ligands must be considered. The $(\mu\text{-SCH}_2\text{CH}(\text{CH}_3)\text{-CH}_2\text{S})[\text{Fe}(\text{CO})_3]_2$ complex, **1**, provides an illustrative example: The down orientation of the methyl group of the S-to-S linker of complex **1** leads to a small energy difference between the most stable rotated form and the most stable unrotated form ($\Delta G = 9.4 \text{ kcal mol}^{-1}$) for the $\text{Fe}(\text{CO})_3$ unit nearest to the methyl group. Complex **1**, however, can rearrange to the lower energy structure **1'** in which the methyl group is oriented up and away from the $\text{Fe}(\text{CO})_3$ units via a low energy transition state which exchanges the axial and equatorial groups of the FeS_2C_3 ring (viz., the exchange of axial and equatorial hydrogens in cyclohexane). The up orientation of the methyl group leads to an energy difference between the most stable rotated form and most stable unrotated form of $12.1 \text{ kcal mol}^{-1}$ for rotation of the $\text{Fe}(\text{CO})_3$ unit nearest to the central methylene hydrogen of complex **1'**. The 2,2-dimethyl-propane-1,3-dithiolate bridge would be more appropriate for generating a stable rotated structure experimentally, because either conformation of this bridge leads to steric repulsion with an apical ligand.

The combination of a sterically demanding dithiolate bridge and asymmetric substitution of strong donor ligands is the most viable method of making better synthetic di-iron complexes that will serve as both structural and functional models of active site of $[\text{FeFe}]_2\text{H}_2\text{ase}$. The amine and borane functionalized complexes stabilize the rotated form but potentially block the site of H^+ acceptance on the self-same iron center.

There are sufficient synthetic precedents for the ready synthesis of the preceding complexes or derivatives thereof. Rauchfuss,^{33,51} Sun,^{23,52} and their respective co-workers have reported the synthesis of a whole range of sterically demanding tertiary amine functionalized dithiolate bridges based on the $(\mu\text{-SCH}_2\text{N}(\text{R})\text{CH}_2\text{S})$ framework and their conversion into the corresponding ammonium salts of the form $(\mu\text{-SCH}_2\text{N}^+\text{-}$

(R)₂CH₂S). Darensbourg,^{13,53} Pickett,^{36,54} Rauchfuss,^{55,56} and their respective co-workers have reported the synthesis of asymmetrically substituted complexes. Our study suggests that the combination of these features into one synthetic

-
- (51) Li, H.; Rauchfuss, T. B. *J. Am. Chem. Soc.* **2002**, *124*, 726–727.
(52) Salyi, S.; Kritikos, M.; Åkermark, B.; Sun, L. *Chem.—Eur. J.* **2003**, *9*, 557–560.
(53) Lyon, E. J.; Georgakaki, I. P.; Reibenspies, J. H.; Darensbourg, M. Y. *Angew. Chem., Int. Ed.* **1999**, *38*, 3178–3180.
(54) Razavet, M.; Davies, S. C.; Hughes, D. L.; Pickett, C. J. *Chem. Commun.* **2001**, 847–848.
(55) Gloaguen, F.; Lawrence, J. D.; Schmidt, M.; Wilson, S. R.; Rauchfuss, T. B. *J. Am. Chem. Soc.* **2001**, *123*, 12518–12527.
(56) Lawrence, J. D.; Li, H.; Rauchfuss, T. B. *Chem. Commun.* **2001**, 1482–1483.

complex will generate a better structural and functional model of the active site of [FeFe]H₂ase.

Acknowledgment. We acknowledge financial support from the National Science Foundation (CHE-0111629 to M.Y.D.; CHE-9800184 and CHE-0518047 to M.B.H.) and R. A. Welch Foundation (A-0924 to M.Y.D.; A-0648 to M.B.H.). We also thank the Supercomputing Facility, the Tensor Beowulf cluster (NSF MRI-0216275), and the Laboratory for Molecular Simulation at Texas A&M University for computer time and software.

IC051231F